Original article

Amir Narimani, Farid Kordnejad, Prabhjyot Kaur, Saeed Bazgir, Mahmood Hemmati and Adam Duong*

Rheological and thermal stability of interpenetrating polymer network hydrogel based on polyacrylamide/hydroxypropyl guar reinforced with graphene oxide for application in oil recovery

https://doi.org/10.1515/polyeng-2021-0147
Received May 18, 2021; accepted July 31, 2021;
published online August 20, 2021

Abstract: The purpose of the present work is to enhance the thermal stability and rheological properties of semi-interpenetrating polymer network (IPN) hydrogel based on partially hydrolyzed polyacrylamide/hydroxypropyl guar (HPAM/HPG) nanocomposite reinforced with graphene oxide (GO), at temperatures (200 and 240 °F) for use in oil recovery applications. FTIR spectra of the IPN nanocomposite hydrogels revealed interactions of GO with HPAM/HPG chains. An increase in the viscosity is also observed from the rheological study. Moreover, IPN and its nanocomposite hydrogels exhibited non-Newtonian behavior. The decline of viscosity of IPN nanocomposite hydrogels was observed with an increase in the temperature from 200 to 240 °F but was still higher than IPN hydrogel without GO. Dispersion of GO through the HPAM/HPG hydrogel matrix was evaluated by SEM morphology and electrical conductivity. The IPN nanocomposite hydrogels showed high viscosity stability, thermal stability, and flow activation energy as compared to IPN hydrogel without GO. Therefore, the addition of 0.1 wt.% of GO to the HPAM/HPG matrix is suitable to create a cross-linked polymer solution with improved properties which may be beneficial for use in oil recovery applications.

Keywords: cross-linked hydrogel; enhanced oil recovery; graphene oxide; rheological behavior; thermal stability.

***Corresponding author: Adam Duong**, Department of Chemistry, Biochemistry, and Physics, Institute de Recherche sur l'Hydrogène, University of Quebec, 3351 boul. des Forges, Trois Rivers, QC G9A 5H7, Canada, E-mail: Adam.Duong@uqtr.ca
Amir Narimani and Prabhjyot Kaur, Department of Chemistry, Biochemistry, and Physics, Institute de Recherche sur l'Hydrogène, University of Quebec, 3351 boul. des Forges, Trois Rivers, QC G9A 5H7, Canada
Farid Kordnejad, Department of Polymer Engineering, Islamic Azad University, South Branch, Tehran, Iran
Saeed Bazgir and Mahmood Hemmati, Department of Petroleum Engineering, Islamic Azad University, Science and Research Branch, Tehran, Iran

1 Introduction

Polymers are often applied in oil recovery applications not only as gel polymers for water production control in-depth reservoir formation, but also for oil displacement in polymer flooding [1, 2]. The hydrophilic polymers boost remarkably the viscosity of the injection water, and decrease the mobility ratio of water to oil, to enhance the sweep efficiency in the reservoir [3, 4]. Polymer solutions present a suitable performance when their viscosity is maintained at the desired level. Therefore, rheological behaviors and properties of the polymer solution play a fundamental role in enhanced oil recovery (EOR) applications. The knowledge of these properties assists in the selecting, designing, and processing of the fluid into porous media like the oil reservoir [5, 6]. Oil reservoirs have a heterogeneous structure with different natural fractures and these reservoirs are also different in terms of porosity and permeability [7], which affects sweep performance [8]. Furthermore, the flow rate corresponds to the shear rate of the polymer solution, which would alter from the well surface to the reservoir [7]. As well, harsh conditions of reservoirs such as salinity and high temperature, affect the stability, and viscosity of polymer solutions during the recovery process [9–11]. Therefore, all these factors can reduce the efficiency of oil recovery [12].

Polyacrylamide (PAM), partially hydrolyzed polyacrylamide (HPAM) [12] xanthan [13], guar [14] are the most important water-dissolvable polymers, used in EOR

applications such as polymer flooding, water shutoff, and also in drilling fluid [11, 15]. HPAM with a cross-linker is mixed to create a gellant that is injected from the surface into the reservoir. Under the effect of temperature and time, HPAM and cross-linker react to make a three-dimensional network structure [16]. However, HPAM is sensitive to salinity, and has poor shear resistance, as well as its molecular chains break while passing through the porous media at high speed [4, 17]. HPAM is also not stable upon increasing the temperature, because of NH_2 group hydrolization [15, 18] which results in a significant decrease in the viscosity and strength of hydrogel. Therefore, to overcome this drawback of hydrogel based on HPAM, mixing with natural polymers, like hydroxypropyl guar (HPG), along with using the chemical cross-linkers through interpenetrating polymer network (IPN) technique can be highly effective [19, 20]. HPG is not only less sensitive to mechanical shearing, but also used as a high modifier in increasing the viscosity [21, 22].

IPN technique is the admixture of two polymers, which have been cross-linked and/or synthesized to improve the new admixture polymer properties. Through this method, various polymer compounds can be prepared based on the desired properties of both polymers by changing their compositions [23, 24]. In addition, when one polymer is cross-linked and the other polymer is not networked, a semi IPN is created. In contrast, when both are cross-linked, a full IPN is created [25]. The present study is limited to the use of semi IPN hydrogel in the presence of the cross-linker as a cross-linked polymer hydrogel. This polymer gel system can flow while having a cross-linked structure in porous media. In fact, cross-linked gel systems can ob viate the difficulty of high permeability zones in a non-homogenous reservoir and enhance control of water production. It can also be used due to the slow-motion of gels in zones with high permeability as an oil displacement by decreasing the mobility ratio as well as reducing the viscous fingering simultaneously [1, 26, 27]. However, the application of this sort of conventional IPN hydrogel as a polymer solution is somewhat limited, because of the low thermal stability of IPN hydrogel that causes reduction of hydrogel viscosity and mechanical performance, especially in reservoirs with high temperatures [10, 12, 19]. Therefore, the mechanical strength, thermal stability, and rheological performance of conventional IPN hydrogel in harsh reservoir conditions can be remarkably improved by the incorporation of nanoparticles owing to their excellent properties, including mechanical strength, salt tolerance, thermal stability, and elasticity [4, 10]. In addition, adding nanoparticles to fluids enhances the effectiveness of oil recovery processes by causing a decline in the interfacial tension and changing the rock wettability [28, 29]. More recently, graphene oxide (GO) has gained attention in this regard and is used as a thermal, electrical, and stiffness reinforcement nanoparticle for hydrogel polymer in harsh conditions [30, 31]. GO is produced by chemical modifying graphene using $KMnO_4$, $NaNO_3$, and H_2SO_4 [32]. It has a large surface area, and also contains abundant functional groups including epoxide, carboxyl, hydroxyl, and carbonyl [33, 34]. Because of its hydrophilic nature and functional groups, it is dispersible in an aqueous environment and is also compatible with some hydrophilic polymers as a modifier [31, 35, 36]. Hence, the major concern to obtain IPN nanocomposite hydrogels with desired viscosity, strength, and thermal stability performance in electrolyte media under harsh reservoir conditions is the uniform dispersion of GO [1, 36, 37].

In this study, IPN nanocomposite hydrogel based on HPAM/HPG, produced by incorporating GO in the presence of chromium triacetate as a cross-linker has been studied. To the best of our knowledge, there is no report on the effect of GO on semi IPN nanocomposite structure based on HPAM/HPG hydrogel system to improve the rheological behavior, thermal stability, and long-term aging of IPN nanocomposite hydrogel for EOR applications. Thus, the purpose of this study is to investigate the influence of GO on the novel semi IPN nanocomposite hydrogel, in terms of viscosity, flow activation energy, temperature, long-term aging, viscosity loss, and thermal stability. In addition, FTIR, morphology, and electrical characterization of nanocomposite hydrogels have been evaluated.

2 Materials and methods

2.1 Materials

HPAM, with 25 mol.% degree of hydrolysis, and 8×10^6 Da molecular weight was supplied by SNF Co. GO (research-grade, Few-Layer: 0.43 gr/cc, Purity: 99%) was obtained from United Nanotech Innovation PVT Ltd, India. HPG with a molecular weight of 2×10^6 Da was obtained from Shandong Shengyou Cementing Engineering & Technology Co., Ltd, China. Chromium triacetate was procured from Carlo Erba, Italy. The total dissolved solids (TDS) of saline water is 7616 ppm.

2.2 Preparation of nanocomposite hydrogels

The IPN hydrogel and nanocomposite hydrogels are prepared and schematically shown in Figure 1. First, 0.35 wt.% of HPAM as well as 0.35 wt.% of HPG powder were gradually added to the separate saline water and stirred regularly by a heater magnetic stirrer to obtain clear viscous solutions at room temperature and aged for 24 h. Then various amounts of GO (0.05, 0.1, 0.3, and 0.5 wt.%) were dispersed in saline

water for 1 h by a magnetic stirrer to form a stable dispersion. Afterwards, the prepared HPG and HPAM were charged in GO solution respectively, and stirring was continued for another 1 h using an overhead mixer (Heidolph RZR 2020). Then, 1.4 wt.% of the chromium triacetate as a cross-linker was prepared in water and added to the aqueous mixture while stirring gently. The reaction mixture was heated at 185 °F (85 °C) for approximately 2 h to obtain a homogeneous solution. The final samples were dried in a vacuum oven for 24 h at 158 °F (70 °C). The polymer concentration of all samples was 0.7 wt.%.

2.3 Characterization

2.3.1 FTIR characterization: Fourier transform infrared (FTIR) spectra were performed by PERKIN ELMER-65 spectrometer, using KBr pellets in the range of 4000–500 cm^{-1}.

2.3.2 Rheological characterization: Rheological characterizations of the nanocomposite hydrogels were performed by a rheometer (Paar-Physica, MCR 301) at temperatures of 200 and 240 °F (93 and 115 °C), which was equipped with parallel plate geometry and also a Peltier device for control of temperature. To inhabit the water loss, silicone oil was used at the outer surface. The strain amplitude was 1% with the frequency in the range 0.01–100 rad/s.

The viscosity stability versus time for the nanocomposite hydrogels was carried out using HT/HP (High temperature/High Pressure) fluid rheology tester (HT/HP Acid-resisting, GRACE M5600 Rheometer). The test of gellant samples was performed for 51 min under a pressure of 480 psi and at the shear rate of 100 1/s. The temperature of the samples was 200 °F and 240 °F.

2.3.3 Morphological characterization: Scanning electron microscopy (SEM) was accomplished by TESCAN Vega Model to study the morphology of HPAM/HPG/GO nanocomposite hydrogels. The fractured surface of samples was coated by sputtering the gold layer.

2.3.4 Electrical characterization: The electrical conductivity of IPN nanocomposite hydrogels was evaluated in conformity with ASTM D257 by Tara S cm^{-1} at 500 V by CEAST Co. The sheet samples (1 mm thick) were prepared and coated with silver paint.

2.3.5 Aging effect: Long-term aging by viscosity monitoring was performed and the samples were held in an oven at 200 and 240 °F, for seven days, separately. The effect of the loss viscosity of these samples on long-term thermal stability was studied.

3 Results and discussion

3.1 FTIR characterization

FTIR was employed to evaluate the interaction between the IPN matrix and GO. As presented in Figure 2, the FTIR spectrum of GO displayed peaks at 3437, 1720, 1623, 1396,

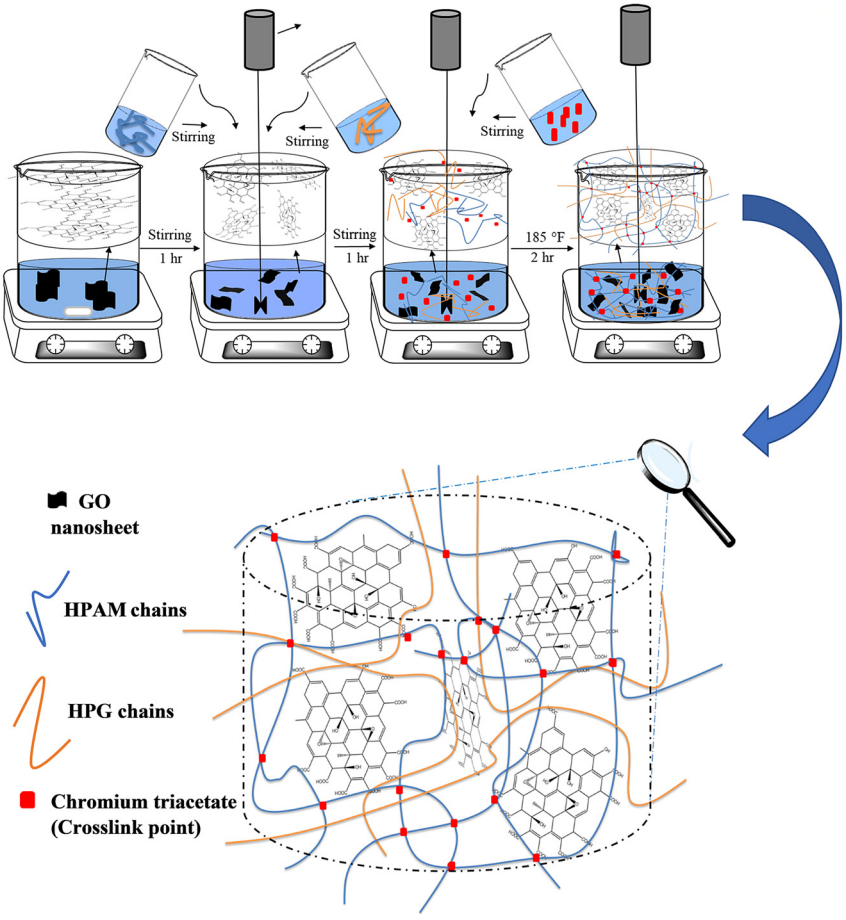

Figure 1: The schematic of the preparation procedure of HPAM/HPG/GO semi IPN nanocomposites hydrogel.

1224, and 1046 cm^{-1}, corresponding to the O–H hydroxyl group, C=O carbonyl stretching, C=C, O–H deformation vibration, C–OH, and C–O–C (epoxy) stretching, respectively [38, 39]. In the spectrum of IPN hydrogel, the peak at 3449 cm^{-1} is attributed to the overlap of the O–H bond of the hydroxyl group of HPG and the N–H band of the amide group of HPAM [21]. Besides, C–H stretching at 2825 cm^{-1} is observed. The peak near 1682 cm^{-1}, is owing to the C=O stretching of the amide group of HPAM. CH_2 scissoring band appears at 1431 cm^{-1}. The peak at 1089 cm^{-1} is due to CH_2–O–CH_2 stretching vibrations. Meanwhile, the peak around 617 cm^{-1} is because of the N–H wagging vibration [21]. By comparing the FTIR spectrums of IPN hydrogel, with nanocomposite hydrogels at 0.1 and 0.5 wt.% of GO, it was observed that most of the characteristic peaks of IPN hydrogel shifted to a lower wavenumber for semi IPN nanocomposite hydrogels. The characteristic peak at 3449 cm^{-1} in HPAM/HPG hydrogel shifted to 3446 and 3445 cm^{-1} in HPAM/HPG/GO for 0.1 and 0.5 wt.% of GO. It indicates that the interaction between GO and matrix occurs by the N-H bond of HPAM in the IPN hydrogel matrix and O–H deformation vibration of GO. The other peaks appear at 2823 and 2824 cm^{-1} for IPN nanocomposites at 0.1 and 0.5 wt.% of GO, indicating the stretching vibration of C–H. Moreover, the characteristic peak in IPN hydrogel moved from 1682 to 1664 and 1662 cm^{-1} for IPN nanocomposites hydrogel at 0.1 and 0.5 wt.% of GO which was related to C=O of the amide group. However, the peak at 1431 cm^{-1} in IPN hydrogel shifted to 1423 and 1422 cm^{-1} for IPN nanocomposite hydrogels at 0.1 and 0.5 wt.% of GO, due to C–H bending vibration. Also, there is the C–O–C stretching around 1085 cm^{-1} for IPN nanocomposites [12, 40]. These results indicate the link between the HPAM/HPG chains and GO through hydrogen bonding [34, 35, 39].

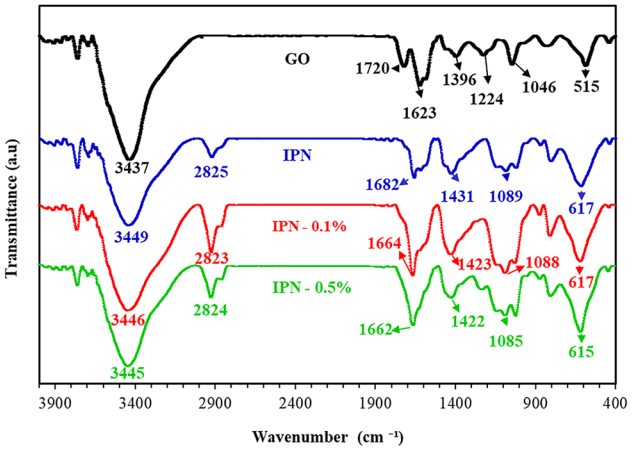

Figure 2: FTIR spectra of GO, IPN (0, 0.1, and 0.5) wt.% of GO.

3.2 Rheological behavior

Polymer flowability is a significant factor in EOR applications because high viscosity polymers solution cannot flow easily in the reservoir, while low viscosity polymers solution decreases polymer injection efficacy in the EOR [2]. To get an insight on this, the dependency of viscosity on the shear rate for IPN nanocomposite hydrogels at 200 and 240 °F was evaluated. As shown in Figure 3, the viscosity was boosted by adding GO, which was remarkable at 0.1 wt.% of GO, at the low shear rate, indicating the formation of physical interaction between GO and the matrix, which restrained the movement of polymer chains, resulting in a rapid rise in the viscosity [12, 41]. In other words, a large surface area of GO nanosheets can act as a multifunctional cross-linker and interact with polymer chains of the matrix, along with the chromium triacetate which created further cross-linking in the polymer network. This leads to an enhancement in the strength of the network structure of nanocomposite hydrogels [35, 42]. Moreover, nanoparticles tend to form agglomerates because of high interparticle interactions [10, 38]. As a result, a slight raise of viscosity was also observed with increasing GO to 0.5 wt.%. According to Figure 3, the viscosity of all samples diminished with a raise in the shear rate. However, the speed of this reduction is related to the GO contents. The nano samples with the addition of GO show better resistance to the increase of shear rate than neat IPN hydrogel, at both temperatures (200 and 240 °F). In fact, GO nanosheet gave greater strength to the IPNs, due to which, the network of IPN nano hydrogel could further withstand against stretch stress and deformation created by shearing fields [42].

It was also found that all samples showed the non-Newtonian and shear thinning behavior, by soaring the shear rate, at both temperatures, which implied the dependency of the power-law to shear rate [11]. This was because of soaring the end-to-end distance as a consequence of unraveling the polymer chains, owing to shear fields. This causes a decrease in polymer viscosity, which implies the pseudoplastic fluid behavior [12]. The shear thinning behavior displays the dependency of rheological properties on the viscoelastic characteristics of the polymer matrix [5].

Figure 4 depicts the influence of GO contents on the viscosity of semi IPN nanocomposite hydrogels for four different shear rates at 200 and 240 °F. At low shear rates (0.1 and 1 1/s), the viscosity soared promptly by adding GO, which was noticeable at 0.1 wt.%, because of the good dispersion of GO into the polymer matrix to form the GO

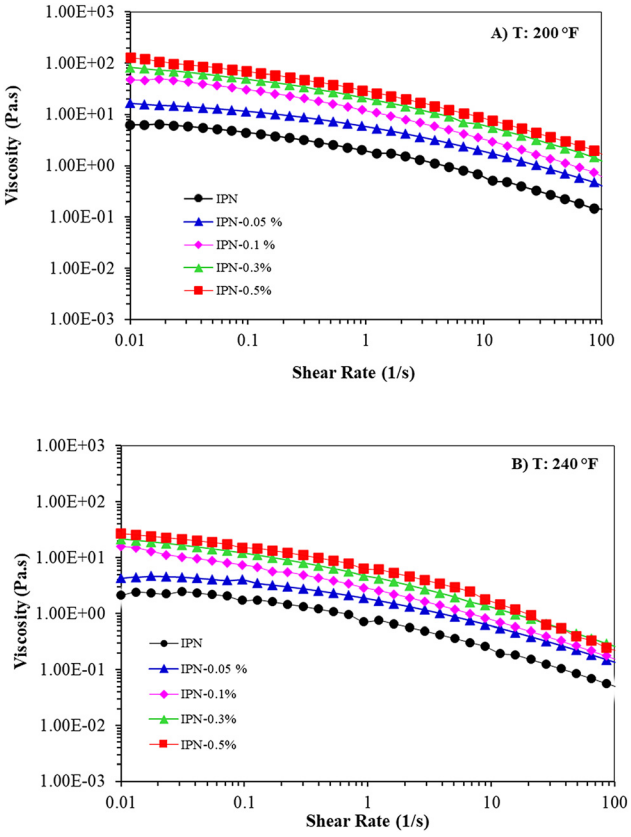

Figure 3: Viscosity versus shear rate of IPN nanocomposite hydrogels at (A) 200 and (B) 240 °F.

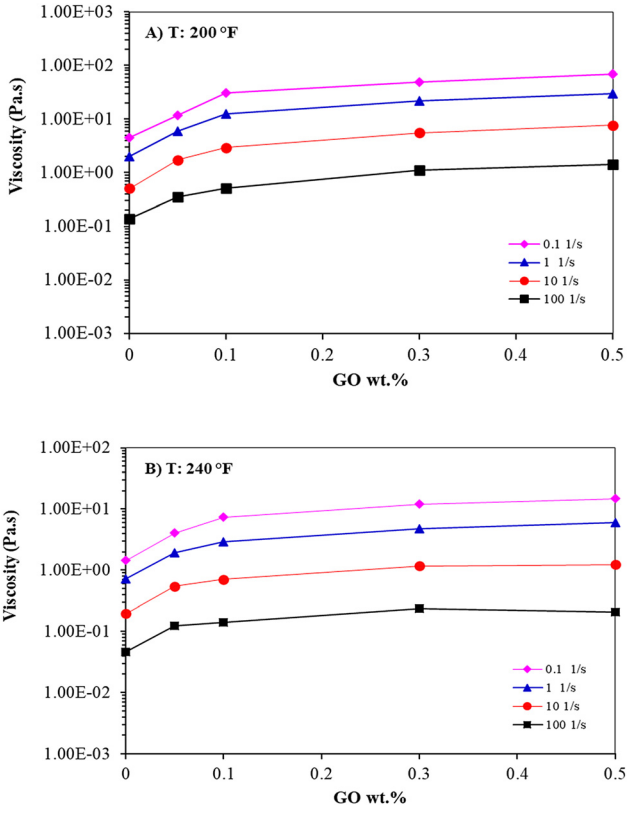

Figure 4: Viscosity versus GO contents at (A) 200 and (B) 240 °F.

network structure. The viscosity continued to increase linearly with an increase in the GO to 0.5 wt.%. In contrast, at a high shear rate (100 1/s), viscosity was less sensitive to the augmentation of GO content. In other words, the reinforcement effect of GO nanosheet was more prevailing at a low shear rate compared to a high shear rate and also at both temperatures 200 and 240 °F [43, 44].

For further understanding of the effect of GO on rheology behavior, the activation energy (E) was studied by the Arrhenius–Frenkel–Eyring equation to appraise the dependency of viscosity to temperature [45] and was computed by Equation (1) [46].

$$\frac{1}{T_1} - \frac{1}{T_2} = \frac{R}{E} \ln\left(\frac{\eta_1}{\eta_2}\right) \tag{1}$$

where η_1, η_2, T_1, T_2, and R were the viscosities, temperatures, and gas constant (8.315 J $gmol^{-1}{\cdot}K^{-1}$), respectively. As shown in Figure 5, the activation energy of the hydrogels reinforced with the addition of 0.1 wt.% of GO. This was mainly attributed to cross-linking between GO as a bridge reinforcer with matrix, causing a resistance to the mobility of the polymer chains, and creating an energetic barrier for polymer chains [9, 47]. In contrast, further increases in GO contents had no suitable effect on flow activation energy.

The common types of polymer degradation are mechanical (shearing) and thermal degradation both of which affect the viscosity of the polymer. However, the effect of temperature is higher than the shear degradation [43]. Polymer solution will expose to diverse temperature gradients from the well surface to the reservoir. Because of this, the effect of temperature on the viscosity of semi IPN nanocomposite hydrogels was investigated. As illustrated in Figure 6, the viscosity diminished with an increase in the temperature from 200 to 240 °F, at all the shear rates. This behavior was due to an increase in chain mobility of polymers and the opening of entanglement of IPN hydrogel chains in the matrix. Moreover, the decrease in the number of cross-linking points into the IPN network at elevated temperatures, and, the undermined strength of the interaction between GO nanosheet and matrix, leads to slippage of polymer chains over GO sheet, causing a decline in the viscosity [5, 10]. However, IPN nanocomposite hydrogel showed great strength, compared to a neat IPN hydrogel because of the GO effect. In other words, when the polymers and GO are dissolved in saline water, the GO as a

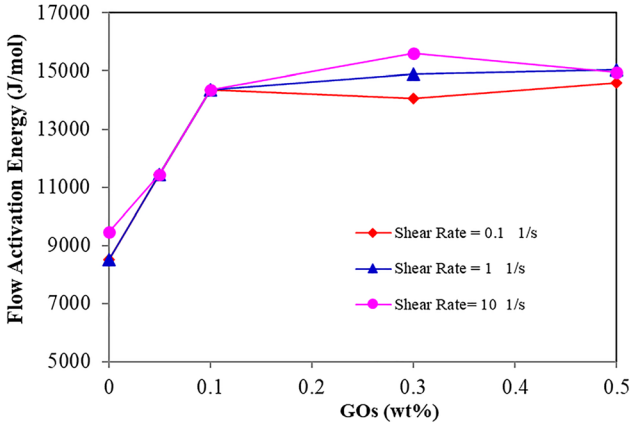

Figure 5: Flow activation energy versus GO contents.

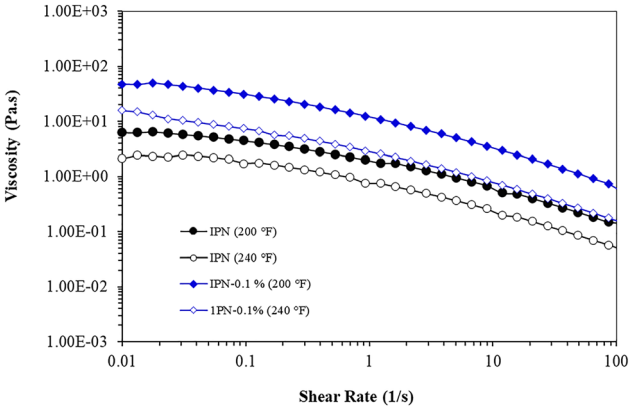

Figure 6: The dependency of the viscosity on the temperature of IPN nanocomposite hydrogels, at 200 and 240 °F.

strong thermal enhancer interacted with polymer chains of IPN hydrogel, to form a durable solution. In addition, functional groups in GO provide cross-linking strength in the hydrogel network. This reinforces the thermal stability of the hydrogel and also reduces the rapid network breakage of the hydrogel with increasing temperatures and shear rates [12, 39]. Besides, the presence of chromium triacetate as a cross-linker can have a positive effect in improving the strength of the IPN network structure [1, 27]. However, despite the presence of a cross-linker in the 'IPN hydrogel without GO', its polymer network would weaken with an increase in temperature, due to the poor strength of cross-linking points, compared to IPN nanocomposites. As a result, cross-linking between polymer chains debilitated, resulting in rapid breakage in its network structure, causing a decrease in the viscosity of the solution [40]. Therefore, GO nanosheets as strong thermal reinforcement can hinder the degradation process and defer the further thermal degradation of the polymer matrix by increasing the temperature [31, 36], which causes the polymer solution to flow further in high permeability zones of a reservoir to ameliorate the oil recovery efficiency.

The viscosity stability of IPN nanocomposite hydrogels is another important rheological parameter in oil recovery and was determined at 200 and 240 °F, and at a constant shear rate of 100 1/s with the time, as shown in Figure 7a and b. Viscosity stability of IPN hydrogel and its nanocomposite hydrogels sharply decreased with time, especially in the first 15 min. The same effect was observed with an increase in temperatures until the arrival at the target temperature (200 and 240 °F). After this, the viscosity remained constant and no significant decline of the viscosity was observed with time under constant shear rate. This viscosity stability was because of the creation of a strong network in the matrix at 0.1 wt.% of GO [48]. However, with a raise in the GO content to 0.5 wt.%, this effect was not significant.

It is also noteworthy from Figure 7c that, the decline in viscosity stability versus the time, at temperature 240 °F was greater than at temperature 200 °F. However, the viscosity stability of the cross-linked polymeric system containing HPAM and HPG hydrogel in the presence of GO at 0.1 wt/% was higher than the HPAM/HPG hydrogel without GO. This behavior was due to the role of GO nanosheet as a reinforcing bridge, leading to an enhancement in the strength of the hydrogel [34, 42]. As a result, the network structure of nanocomposite hydrogels displayed shear stability and also required more shear force and time to break its strength.

3.3 Morphological characterization

To better understand the dispersion of GO for IPN hydrogels, the morphology of the nanocomposite hydrogels was evaluated by SEM. As observed in Figure 8a–c, GO is well dispersed in a mixture solution of HPAM and HPG and formed a uniform solution with the addition of 0.1 wt.% and somewhat uniform at 0.3 wt.% while some agglomerate of the GO particles was observed with the further increase in GO to 0.5 wt.%, as shown in Figure 8d. This was due to the strong interparticle attraction of GO to form agglomerates in the matrix of IPN hydrogel [49, 50]. In addition, GO particles trend the sedimentation in solution [18], which may cause plugging of the pores in the reservoir, due to nonuniformed dispersions and sedimentation of particles [51]. Therefore, the GO concentration is the key factor for the performance of the interpenetrated polymer network.

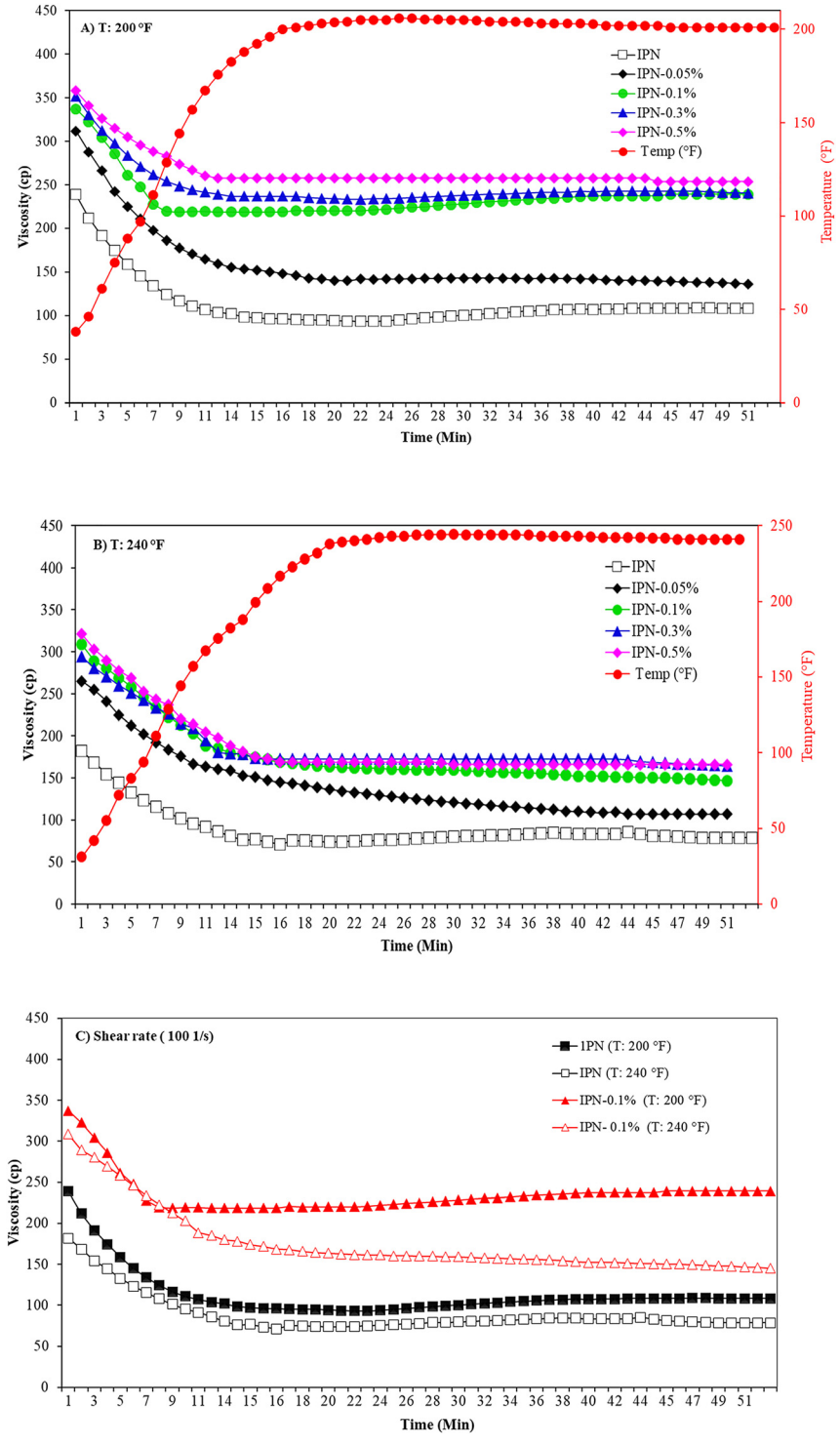

Figure 7: The influence of time on the viscosity stability of IPN nanocomposite hydrogels at (A) 200 °F, (B) 240 °F, and (C) shear rate at 100 1/s.

3.4 Electrical characterization

For further evaluation of the dispersion of GO in the IPN hydrogel systems, the electrical conductivity of IPN nanocomposite hydrogels was also investigated. As can be observed in Figure 9, with the addition of GO up to 0.1 wt.%, the conductivity of nanocomposite increased, this change in electrical conductivity was due to the good dispersion of GO nanosheets within the IPN matrix, to form a strong network structure. As a result, a large number of the electrons are transported within the matrix, owing to the creation of the interconnecting conductive channels [31, 50]. Moreover, this

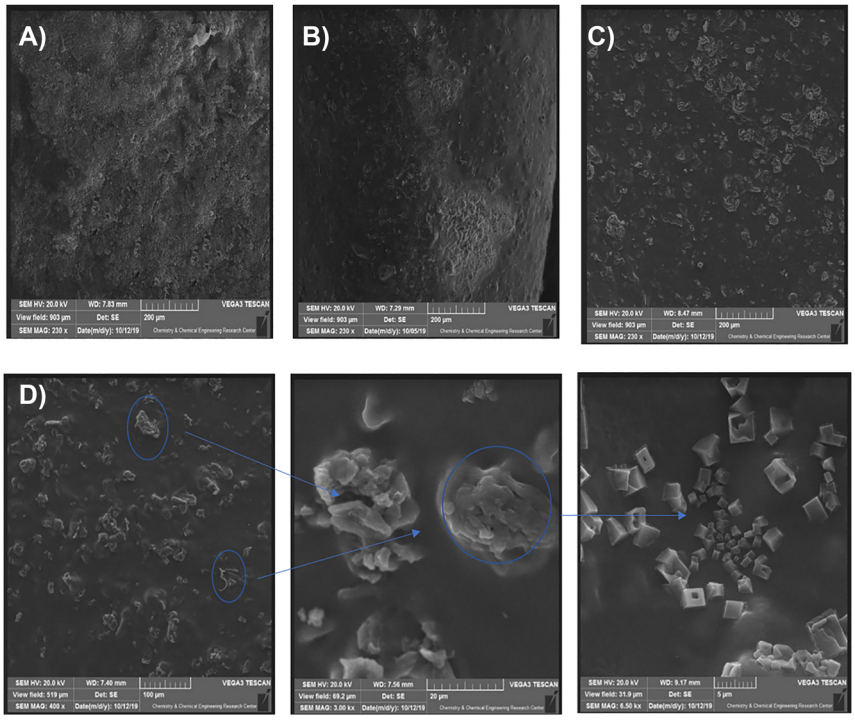

Figure 8: SEM images of IPN nanocomposites hydrogel: (A) 0.1, (B) 0.3, (C) 0.5 wt.% of GO, and (D) agglomeration of GO particles at 0.5 wt.%.

raise in electrical conductivity corresponded to the formation of stable conductivity paths [31]. However, electrical resistivity decreased when GO contents increased up to 0.5 wt.%. This may be due to poor GO dispersion and decline in the distance between the GO sheets with increasing GO contents. This leads to a decrement in the passing of electrons through the matrix and hinders the formation of the electrical network, indicating an agglomerate of GO particles in the IPN matrix [52]. Therefore, the electrical conductivity of IPN nanocomposite hydrogels improved by reinforcing the effect of GO but up to 0.1 wt.% of GO. This behavior was also supported by morphology and rheological studies.

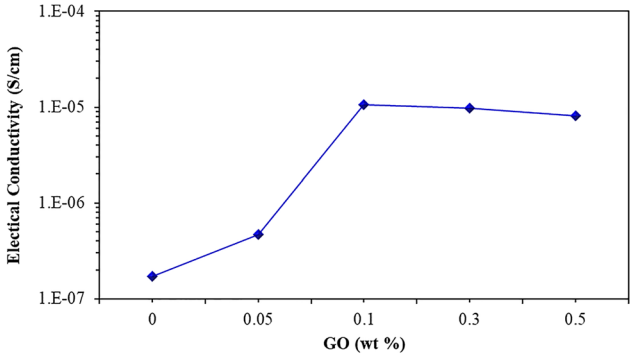

Figure 9: Electrical conductivity versus GO contents.

3.5 Aging effect

Viscosity loss of polymer solutions is a significant element in polymer injection, especially in long-term aging under harsh conditions of the reservoir in EOR applications. Because of this, the influence of thermal aging on the viscosity behavior of IPN nanocomposite hydrogels, at temperatures of 200 and 240 °F were investigated. As highlighted in Figure 10, the shear viscosity of all samples decreases remarkably by increasing shear rate and temperature. This reduction of viscosity was dependent on GO concentration. Indeed, the physical interaction between GO and matrix undermined significantly, resulting in a decrease in the strength of the IPNs network structure [11]. Interestingly, with the addition of GO to 0.1 wt.%, the sample displayed higher thermal stability than all samples. This behavior is because of the good dispersion of GO in the IPN hydrogel matrix and makes a potent physical interaction with HPAM and HPG chains [10, 18]. Besides, the presence of chromium triacetate and HPG in the matrix further strengthens the IPN network and improves the shear stability [1, 21, 22]. In addition, the cross-linked network of polymer solutions caused decreasing accessibility of divalent cations such as Ca^{2+} and Mg^{2+} to the HPAM chains [2], and the polymer solution presenting greater thermal stability. According to this result, the GO nanosheet as a reinforcing bridge enhanced

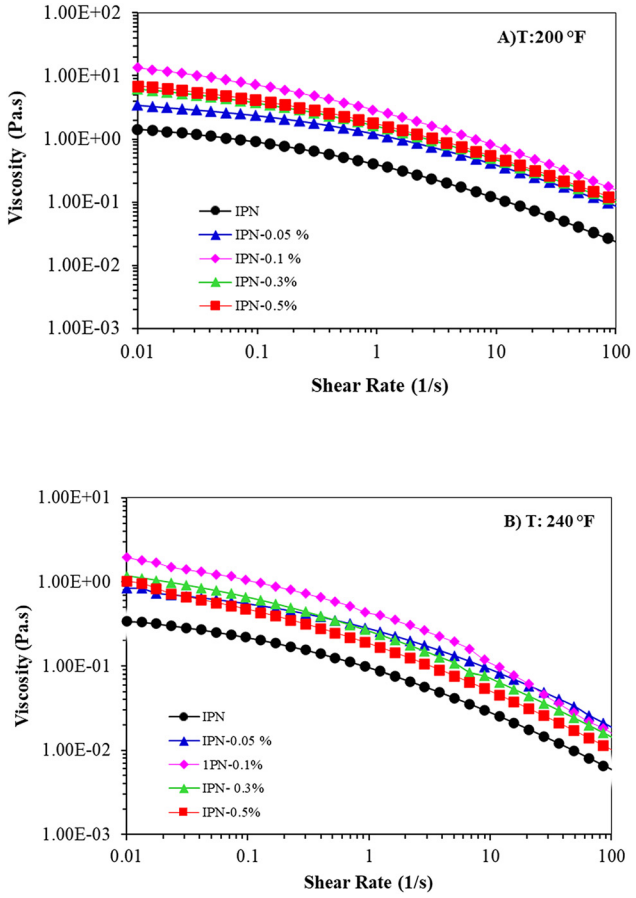

Figure 10: Viscosity vs. shear rate of IPN nanocomposite hydrogels after aging at (A) 200 °F and (B) 240 °F.

the strength of the IPN network and boosted the thermal stability and viscosity stability of the polymer solution at high temperatures for the long-term. In contrast, with an increase in the GO contents up to 0.5 wt.%, viscosity decreased. This effect could be due to the formation of the agglomerate of GO, which notably reduced the interaction between GO and matrix, because of a decline in the cross-linking in the network. This behavior was supported by morphological studies. Therefore, based on these results, IPN nanocomposite hydrogel by adding 0.1 wt.% of GO, showed less viscosity loss than the other samples at both temperatures, for long-term aging.

4 Conclusion

Rheological and thermal aging of IPNs based on partially HPAM/HPG reinforced by GO was investigated at various temperatures. The dependency of GO on improving the thermal and viscosity stability was relevant to the good dispersion of GO and its interaction with polymer chains. The interaction of GO with HPAM/HPG chains of IPN hydrogel was observed by FTIR spectra. The rheological studies demonstrated that the viscosity increased by increasing GO contents, while it diminished with the rise in the shear rate, indicating the shear thinning behavior. GO enhanced viscosity stability of nano samples with an increase in temperature from 200 to 240 °F, and improved the nanocomposite hydrogel effects, compared to the IPN hydrogel without GO. Flow activation energy elevated by adding 0.1 wt.% of GO. Rheological and morphology results were sensitive to the physical interaction between GO and matrix. SEM study showed the enhancement of the dispersion of GO in the matrix of the polymer (HPAM/HPG) at 0.1 wt.%. This effect is followed by electrical conductivity that improved at 0.1 wt.%. Nano samples exhibited viscosity stability behavior and mechanical strength, at both temperatures 200 and 240 °F, under constant shear rate. GO enhanced the thermal stability of HPAM/HPG/GO hydrogel in long-term thermal aging, compared to IPN hydrogel. Therefore, it can be concluded from these results that the PHPA/HPG/GO nanocomposite hydrogel presents suitable thermal and viscosity stability which may be beneficial for use in a high temperature reservoir.

Author contributions: All the authors have accepted responsibility for the entire content of this submitted manuscript and approved submission.

Research funding: This study was funded by the Natural Sciences and Engineering Research Council of Canada (RGPIN-2015-06425), the Canadian Foundation for Innovation (Grant number: 37843), and the Université du Québec à Trois-Rivières.

Conflict of interest statement: The authors have no conflicts of interest to declare regarding this article.

References

1. Wang W., Liu Y., Gu Y. Application of a novel polymer system in chemical enhanced oil recovery (EOR). *Colloid Polym. Sci.* 2003, *281*, 1046–1054.
2. Alvand E., Aalaie J., Mahmood H., Sajjadian V. A. Thermal stability adsorption and rheological behaviors of sulfonated polyacrylamide/chromium triacetate/laponite nanocomposite weak gels *Macromol. Res.* 2017, *25*, 27–37.
3. Zhu S., Shi L., Wang X., Liu C., Xue X., Ye Z. Investigation into mobility control mechanisms by polymer flooding in the offshore high-permeable heavy oil reservoir *Energy Sources, Part A Recovery, Util. Environ. Eff.* 2020, 1–14; https://doi.org/10.1080/15567036.2020.1797941.
4. Cheraghian S., Hendraningrat L. A review on applications of nanotechnology in the enhanced oil recovery part A: effects of nanoparticles on interfacial tension. *Int. Nano Lett.* 2016, *6*, 129–138.

5. Aalaie J. Rheological behavior of polyacrylamide/laponite nanoparticle suspensions in electrolyte media. *J. Macromol. Sci. Part B: Phys.* 2012, *51*, 1139–1147.
6. Dang T. Q. C., Chen Z., Nguyen T. B. N., Bae W. Rheological modeling and numerical simulation of HPAM polymer viscosity in porous media. *Energy Sources, Part A* 2015, *37*, 2189–2197.
7. Van den Hoek P. J. Impact of induced fractures on sweep and reservoir management in pattern floods. In *SPE-90968-MS; SPE annual technical conference and exhibition*; Society of Petroleum Engineers: Houston, USA, 2004.
8. Shedid A. Influences of fracture orientation on oil recovery by water and polymer flooding processes: an experimental approach. *J. Petrol. Sci. Eng.* 2006, *50*, 285–292.
9. Kamal M. S., Hussien I. A., Abdullah S. S., Han M. Rheological study on ATBS-AM copolymer-surfactant system in high-temperature and high-salinity environment *J. Chem.* 2013, 1–9; https://doi.org/10.1155/2013/801570.
10. Hu Z., Haruna M., Gao H., Nourafkan E. Rheological properties of partially hydrolyzed polyacrylamide seeded by nanoparticles. *J. Ind. Eng. Chem.* 2017, *56*, 3456–3463.
11. Wei B., Rodrigue D. Mechanical properties, and flow behavior of polymers for enhanced oil recovery. *J. Macromol. Sci. Part B: Phys.* 2014, *53*, 625–644.
12. Haruna M. A., Pervaiz S., Hu Z., Nourafkan E., Wen D. Improved rheology and high-temperature stability of hydrolyzed polyacrylamide using graphene oxide nanosheet. *J. Appl. Polym.* 2019, *47582*, 1–13.
13. Mothe C. G., Correia D. Z., Franca F. P., Riga A. T. Thermal and rheological study of polysaccharides for enhanced oil recovery. *J. Therm. Anal. Calorim.* 2006, *85*, 31–36.
14. Wang S., Tang H., Guo J., Wang K. Effect of pH on the rheological properties of borate crosslinked hydroxypropyl guar gum hydrogel and hydroxypropyl guar gum. *Carbohydr. Polym.* 2016, *147*, 455–463.
15. Jiang C., Xia X., Kang S., Dong H., Sakinejad P., Ma Q., Tang Y. Neighboring group effect on the thermal degradation of polyacrylamide and its derivatives. *J. Polym. Eng.* 2019, *39*, 239–247.
16. Elkarsani K. S. M., Al-Muntasheri G. A., Sultan A. S., Hussein I. A. Performance of PAM/PEI gel System for water shutoff in high-temperature reservoirs: laboratory study. *J. Appl. Polym. Sci.* 2015, *132*, 1–10.
17. Li F., Zhua W. X., Yu D. Z., Song H., Wang K. L. Rheological properties and enhanced oil recovery performance of a novel sulfonate polyacrylamide. *J. Macromol. Sci, Pure Appl. Chem.* 2018, *55*, 449–454.
18. Haruna M. A., Gardy J., Yao G., Hu Z., Hondow N., Wen D. Nanoparticle modified polyacrylamide for enhanced oil recovery at harsh conditions. *Fuel* 2020, *268*, 1–19.
19. Erdlac R. J., Armour L., Lee R., Snyder S., Sorensen M., Matteucci M., Horton J. *Processing of Thirty-Second Workshop on Geothermal Reservoir Engineering*; Stanford University: Stanford, California, USA, 2007; pp. 22–24.
20. Yahya G. O., Ali S. A., Al-Naafa M. A., Hamad E. Z. Preparation and viscosity behavior of hydrophobically modified poly vinyl alcohol (PVA). *J. Appl. Polym. Sci.* 1995, *57*, 343–352.
21. Nayak B. R., Singh R. P. Development of graft copolymer flocculating agents based on hydroxypropyl guar gum and acrylamide. *J. Appl. Polym. Sci.* 2001, *81*, 1776–1785.
22. Zhu J., Guan S., Hu Q., Gao G., Xu K., Wang P. Tough, and pH-sensitive hydroxypropyl guar gum/polyacrylamide hybrid double-network hydrogel. *Chem. Eng. J.* 2016, *306*, 953–960.
23. Budianto E., Amalia A. Swelling behavior and mechanical properties of Chitosan-Poly(N-vinyl-pyrrolidone) hydrogels. *J. Polym. Eng.* 2020, *40*, 551–560.
24. Rahmatpour A., Soleimani P. Synthesis and characterization of novel semi-IPN nanocomposite hydrogels based on guar gum, partially hydrolyzed poly(acrylamide), and pristine montmorillonite *Polym. Bull.* 2020; https://doi.org/10.1007/s00289-020-03408-9.
25. Kheirabadi M., Bagheri R., Kabiri K. Swelling and mechanical behavior of nanoclay reinforced hydrogel: single network vs. full interpenetrating polymer network. *Polym. Bull.* 2015, *72*, 1663–1681.
26. Alvand E., Aalaie J., Hemmati M., Sajjadian V. A. Rheological and thermal stability of novel weak gels based on sulfonated polyacrylamide/scleroglucan/chromium triacetate. *Polym. Int.* 2016, *66*, 477–484.
27. Sun F., Lin M., Dong Z., Zhu D., Wang S. L., Yang J. Effect of composition of HPAM/chromium (III) acetate gels on delayed gelation time. *J. Dispersion Sci. Technol.* 2016, *37*, 753–759.
28. Cheraghian S., Hendraningrat L. A review on applications of nanotechnology in the enhanced oil recovery part B: effects of nanoparticles on flooding. *Int. Nano Lett.* 2016, *6*, 1–10.
29. Aliabadiana E., Sadeghia S., Moghaddam A. R., Mainia B., Chena Z., Sundararaja U. Application of graphene oxide nanosheets and HPAM aqueous dispersion for improving heavy oil recovery: effect of localized functionalization. *Fuel* 2020, *265*, 116918.
30. Chen J. Y., Xie P., Zhang Z. P. Reduced graphene oxide/polyacrylamide composite hydrogel scaffold as biocompatible anode for microbial fuel cell. *Chem. Eng. J.* 2019, *361*, 615–624.
31. Liu X., Shao X. Y., Fang G. B., Hai H., Wan Z. G. Preparation, and properties of chemically reduced graphene oxide/copolymer-polyamide nanocomposite hydrogels. *E-Polymers* 2017, *17*, 3–14.
32. Hummers W. S., Offeman R. E. Preparation of graphitic oxide *J. Am. Chem. Soc.* 1985, *80*, 1339.
33. Manivel P., Kanagaraj S., Balamurugan A., Ponpandian N., Mangalaraj D., Viswanathan C. Rheological behavior-electrical and thermal properties of polypyrrole/graphene oxide nanocomposite hydrogels. *J. Appl. Polym. Sci.* 2014, *131*, 1–10.
34. Fan J., Shi Z., Lian M., Li H., Yin J. Mechanically strong graphene oxide/sodium alginate/polyacrylamide nanocomposite hydrogel with improved dye adsorption capacity. *J. Mater. Chem. A.* 2013, *1*, 7433–7443.
35. Kheirabadi M., Bagheri R., Kabir K., Ossipov D., Jokar E., Asadian E. Improvement in mechanical performance of anionic hydrogels using full-Interpenetrating polymer network reinforced with graphene oxide nanosheets. *Adv. Polym. Technol.* 2016, *35*, 1–10.
36. Nguyen B. D., Ngo T. K., Bui T. H., Pham D. K., Dinh X. L., Nguyen P. T. The impact of graphene oxide particles on viscosity stabilization for diluted polymer solutions using in enhanced oil recovery at HTHP offshore reservoirs *Adv. Nat. Sci. Nanosci. Nanotechnol.* 2015, *6*, 1–8.
37. Lee K. S. The Effects of the shear-thinning property of injection fluid on the performance of polymer flood. *Energy Sources, Part A.* 2013, *35*, 1550–1559.

38. Moazzami M., Sharif F. Enhancement of dispersion and bonding of graphene-polymer through wet transfer of functionalized graphene oxide. *Express Polym. Lett.* 2012, *6*, 1017–1031.
39. Zhang H., Zhai D., He Y. Graphene oxide/polyacrylamide/carboxymethyl cellulose sodium nanocomposite hydrogel with enhanced mechanical strength: preparation, characterization and the swelling behaviors. *RSC Adv.* 2014, *4*, 44600–44609.
40. Liu R., Liang S., Tang X. Z., Yan D., Li X., Yu Z. Z. Tough and highly stretchable graphene oxide/polyacrylamide nanocomposite hydrogels. *J. Mater. Chem.* 2012, *22*, 14160–14167.
41. Haraguchi K., Takehisa T., Fan S. Effects of clay content on the properties of nanocomposite hydrogels composed of poly (N-isopropyl acryl amide) and clay. *Macromolecules* 2002, *35*, 10162–10171.
42. Tarash S., Nazockdast H., Sodeifian G. Reinforcing effect of graphene oxide on mechanical properties, self-healing performance, and recoverability of double network hydrogel based on k-carrageenan and polyacrylamide. *Polymer* 2019, *183*, 121837.
43. Cheraghian G., Khalili Nezhad S., Bazgir S. Improvement of thermal stability of polyacrylamide solution used as a nano-fluid in enhanced oil Recovery process by nano clay *Int. J. Nanosci. Nanotechnol.* 2015, *11*, 201–208.
44. Seo M. K., Park S. J. Electrical resistivity and rheological behavior of carbon nanotubes-filled polypropylene composites. *Chem. Phys. Lett.* 2004, *395*, 44–48.
45. Narimani A., Hemmati M. Study on the electrical and rheological percolation threshold of single-walled carbon nanotube-reinforced thermoplastic elastomer based on polypropylene/ethylene–propylene–diene monomer nanocomposite. *J. Thermoplast. Compos. Mater.* 2015, *28*, 930–949.
46. Dealy J. M., Wissbrun K. F. *Melt Rheology and Its Role in Plastics Processing*; Chapman & Hall: London, 1996.
47. Rahmatpour A., Aalaie J. Steady shear rheological behavior, mechanical properties, and morphology of the polypropylene/carbon nanotube nanocomposites. *J. Macromol. Sci. Part B: Phys.* 2008, *47*, 929–941.
48. Jiang C., Yu B., Ma Q., Dong H., Zhao H., Luo Y., Tang Y. Crosslinked polymers as "smart" viscosifiers used in hostile environments. *J. Petrol. Sci. Eng.* 2019, *173*, 1332–1339.
49. Zhong C., Luo P., Ye Z. Characterization and solution properties of a novel water-soluble terpolymer for enhanced oil recovery. *Polym. Bull.* 2009, *62*, 79–89.
50. Zhou T. N., Qi X. D., Fu Q. The preparation of the poly (vinyl alcohol)/graphene nanocomposite hydrogels with low percolation threshold and high electrical conductivity by using the large-area reduced graphene oxide sheets. *Express Polym. Lett.* 2013, *7*, 747–755.
51. Sharma T., Velmurugan V., Patel P., Chon B. H., Sangwai J. S. Use of oil-in-water pickering emulsion stabilized by nanoparticles in combination with polymer flood for enhanced oil recovery. *Petrol. Sci. Technol.* 2015, *33*, 1595–1604.
52. Sung Y. T., Han M. S., Song H., Jung J. W., Lee H. S. Rheological and electrical properties of polycarbonate MWCN composites. *Polymer* 2006, *47*, 4434–4439.